Hindawi Publishing Corporation
EURASIP Journal on Wireless Communications and Networking
Volume 2010, Article ID 164651, 12 pages
doi:10.1155/2010/164651

Research Article

Frame-Aggregated Link Adaptation Protocol for Next Generation Wireless Local Area Networks

Kai-Ten Feng, Po-Tai Lin, and Wen-Jiunn Liu

Department of Electrical Engineering, National Chiao Tung University, Hsinchu 300, Taiwan

Correspondence should be addressed to Kai-Ten Feng, ktfeng@mail.nctu.edu.tw

Received 4 August 2009; Revised 11 February 2010; Accepted 10 May 2010

Academic Editor: Ashish Pandharipande

The performance of wireless networks is affected by channel conditions. Link Adaptation techniques have been proposed to improve the degraded network performance by adjusting the design parameters, for example, the modulation and coding schemes, in order to adapt to the dynamically changing channel conditions. Furthermore, due to the advancement of the IEEE 802.11n standard, the network goodput can be enhanced with the exploitation of its frame aggregation schemes. However, none of the existing link adaption algorithms are designed to consider the feasible number of aggregated frames that should be utilized for channel-changing environments. In this paper, a frame-aggregated link adaptation (FALA) protocol is proposed to dynamically adjust system parameters in order to improve the network goodput under varying channel conditions. For the purpose of maximizing network goodput, both the optimal frame payload size and the modulation and coding schemes are jointly obtained according to the signal-to-noise ratio under specific channel conditions. The performance evaluation is conducted and compared to the existing link adaption protocols via simulations. The simulation results show that the proposed FALA protocol can effectively increase the goodput performance compared to other baseline schemes, especially under dynamically-changing environments.

1. Introduction

A wireless network is a type of computer networks that utilizes wireless communication technologies to maintain connectivity and exchange messages between stations over wireless media, such as infrared, laser, ultrasound, and radio waves. Due to the wireless nature, wireless networks possess many advantages against its wired counterpart, for example, capable of device mobility, simple installation, and ease of deployment. Depending on the coverage, wireless networks can in general be divided into five different categories, including wireless regional area networks (WRANs), wireless wide area networks (WWANs), wireless metropolitan area networks (WMANs), wireless local area networks (WLANs), and wireless personal area networks (WPANs). The IEEE standards association establishes five standard series of IEEE 802.22, 802.20, 802.16, 802.11, and 802.15 for the corresponding networks. Among these wireless standard series, the IEEE 802.11 standard is considered the well-adopted suite for WLANs due to its remarkable success in both design and deployment.

In recent years, the IEEE 802.11 standard has been used both for indoor and mobile communications. The applications for WLANs include wireless home gateways, hotspots for commercial usages, and ad hoc networking for intervehicular communications. Various amendments are contained in the IEEE 802.11 standard suite, mainly including IEEE 802.11a/b/g [1–3], IEEE 802.11e [4] for quality-of-service (QoS) support. With the increasing demands to support multimedia applications, the new amendment IEEE 802.11n [5, 6] has been proposed for achieving higher goodput performance. The IEEE 802.11 task group N (TGn) enhances the PHY layer data rate up to 600 Mbps by adopting advanced communication techniques, such as orthogonal frequency-division multiplexing (OFDM) and multiinput multioutput (MIMO) technologies [7]. It is noted that MIMO technique utilizes spatial diversity to improve both the range and spatial multiplexing for achieving higher data rate. However, it has been investigated in [8] that simply improves the PHY data rate will not be suffice for enhancing the system goodput from the medium access control (MAC) perspective. Accordingly, the IEEE 802.11

TGn further exploits frame aggregation and block acknowledgment techniques [9] to moderate the drawbacks that are originated from the MAC/PHY overheads.

There is research work proposed in [10–19] that focus on packet aggregation schemes for WLANs. Two-level aggregation techniques, that is, the aggregate MAC service data unit (A-MSDU) and the aggregate MAC protocol data unit (A-MPDU), are exploited in the current IEEE 802.11n draft. Performance comparisons between IEEE 802.11, 802.11e, and 802.11n protocols have been presented in [10]. The benefits of adopting two-level packet aggregation have been shown in [11, 12] for the enhancement of network goodput; while experimental studies on packet aggregation were conducted in [13]. Feasible fragmentation and retransmission of packets has been studied in [15, 16] for goodput enhancement with the consideration of contending stations [14]. It has been suggested in [17] to adopt packing, concatenation, and multiple frame transmission in order to reduce the MAC/PHY overheads. For goodput enhancement of VoIP traffic, Lu et al. [18] recommended the MAC queue aggregation (MQA) scheme; while Lee et al. [19] exploits intercall aggregation for multihop networks. Nevertheless, most of the existing schemes do not consider the effectiveness of packet aggregation techniques under time-varying channel conditions.

On the other hand, in order to improve the network performance within dynamically changing environments, link adaptation techniques are proposed by adjusting major design parameters according to the channel conditions, for example, based on the signal-to-noise ratio (SNR) values. The automatic rate fallback (ARF) algorithm as developed in [20] regulates the packet transmission rate based on the available feedback information from the acknowledgment (ACK) frames. Due to the severe delay problems encountered by the ARF scheme under highly varying channel conditions, cross link adaptation (CLA) algorithms [21–23] are proposed to alleviate the degraded network goodput. A mapping table between the SNR value and the modulation and coding scheme (MCS) is pre-established by the CLA algorithms, where an optimal MCS scheme is obtained in order to maximize the saturated network goodput. However, none of the existing link adaptation algorithms is specifically designed under the scenarios with frame aggregation. It will be beneficial to provide an efficient link adaptation scheme such as to enhance the system goodput for the IEEE 802.11n networks.

In this paper, a frame-aggregated link adaptation (FALA) protocol is proposed to maximize the goodput performance for the IEEE 802.11n networks based on cross-layer information. The conventional rate-adaptive schemes simply consider the choice of the PHY-layer modulation and coding schemes (MCS) in the goodput modeling. Therefore, in order to further enhance the network goodput performance, the proposed FALA algorithm additionally adopts the MAC-layer frame payload size as another degree of freedom to theoretically model the system goodput. Moreover, the A-MPDU/A-MSDU frame aggregation scheme adopted in the IEEE 802.11n MAC protocol is also taken into account under the saturated goodput performance. According to the results obtained from the goodput analysis, a table containing both the optimal MCS scheme and optimal MPDU payload size will be pre-established in order to facilitate the implementation of the proposed FALA algorithm. After acquiring the SNR value from the communication channel, an appropriate combination of both the MCS scheme and the frame payload size will be selected in order to maximize the network goodput. Simulations are also implemented to evaluate the effectiveness of the proposed FALA algorithm under the existence of channel variations. Compared with other baseline schemes, higher MCS can be utilized by the proposed FALA protocol under the same signal-to-noise condition, which can be observed that the FALA scheme outperforms other existing link adaptation algorithms with improved network goodput.

The remainder of this paper is organized as follows. Section 2 describes existing link adaptation algorithms. The proposed FALA protocol associated with the goodput analysis is presented in Section 3. Section 4 provides the performance evaluation of the proposed FALA scheme; while the conclusions are drawn in Section 5.

2. Preliminaries

The mechanism of link adaptation denotes the concept of establishing the mapping between the modulation, coding, or other protocol parameters toward the channel conditions. Two well-adopted link adaptation algorithms, that is, the ARF and the CLA schemes, are briefly summarized as follows. Both schemes will be evaluated and compared via simulations in Section 4.

2.1. Automatic Rate Fallback (ARF) Algorithm. The ARF scheme in [20] determines the required packet transmission rate based on the success of transmission attempts. Two counters are utilized to trace the consecutively received correct and missed ACK frames, respectively, which are adopted to reflect the corresponding channel conditions. If the successive ACK frames that are correctly received have reached the number of ten, the packet transmission rate for next transmission attempt will be upgraded to a higher-level rate. On the other hand, as the number of consecutively missed ACK frames reaches two, the packet transmission rate will fallback to a lower-level rate. The advantage of adopting the ARF algorithm is its simple computation which only involves the design of several counters and timers within the MAC layer protocol. However, without the consideration of PHY layer information (e.g., the channel SNR values), the adaptation scheme within the ARF protocol is in general insensitive to the channel variations. As the degree of channel variation is raised, considerable delayed performance will be incurred by exploiting the ARF algorithm.

2.2. Cross-Layer Link Adaptation (CLA) Algorithm. In order to alleviate the problem as described in the ARF scheme, the CLA algorithm [21] associated with its derivative schemes [22, 23] are proposed by incorporating PHY layer information for the MAC protocol design. The saturated goodput

analysis of the IEEE 802.11 distributed coordination function (DCF) is utilized for the determination of transmission rate within the CLA algorithm. For achieving the maximal goodput performance, a mapping table is established to obtain an optimal MCS scheme based on a given channel SNR value. It is noted that this mapping table is constructed offline, and will be served as a realtime lookup table for each device to obtain a feasible MCS scheme under specific channel condition. Owing to the online mapping from the SNR value to the corresponding optimal MCS scheme, the goodput performance by adopting the CLA scheme can be greatly improved, especially under severe channel variation.

3. Proposed Frame-Aggregated Link Adaptation (FALA) Protocol

By using the PHY layer information, it is intuitive that the CLA scheme should result in enhanced goodput performance compared to the ARF algorithm under channel variations. Considering the protocol design for IEEE 802.11n standard, it can be beneficial to incorporate the frame aggregation within the link adaptation scheme in order to maximize the network goodput. Section 3.1 discusses the observations that are acquired from the goodput characteristics of IEEE 802.11n protocol. The saturated goodput analysis with the consideration of frame aggregation is described in Section 3.2; while the implementation of proposed FALA protocol is explained in Section 3.3.

3.1. Goodput Observation based on IEEE 802.11n Protocol. Except for the main features of MIMO and OFDM techniques, multiple packet transmission rates are also provided in the IEEE 802.11n PHY standard through the utilization of different MCS schemes, including both the modulation modes and coding rates. Furthermore, the IEEE 802.11n MAC protocol mandates the implementation of frame aggregation scheme for the sake of promoting the transmission efficiency. With the frame aggregation scheme as shown in Figure 1, multiple MAC protocol data units (MPDUs) are combined into an aggregated MPDU (A-MPDU), which is consequently transported into a single PHY service data unit (PSDU). Moreover, the MPDU payload within each MPDU can be designed to consist multiple service data units (MSDUs), which results in the A-MSDU as in Figure 1. Intuitively, the transmission efficiency can be improved with the usage of A-MPDU and/or A-MSDU since more data units are transmitted with a communion of control overhead.

In order to observe the effect from the number of aggregated frames to the goodput performance, performance comparison via simulations obtained from [15, 16] has been rerun as shown in Figure 2. Considering different bit error rate (BER) values, the goodput performance under different numbers of aggregated MPDUs is shown in Figure 2(a); while that with different numbers of aggregated MSDUs is illustrated in Figure 2(b). It can be seen that the network goodput is increased along with the incremented number of MPDUs. However, the network goodput will reach a maximal value and decrease as the number of aggregated

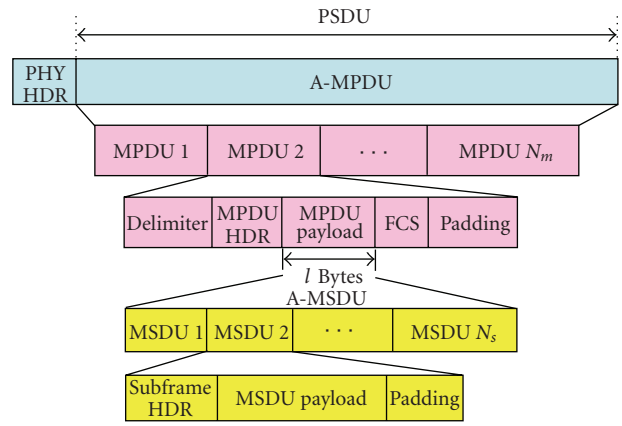

Figure 1: The schematic diagram of A-MPDU and A-MSDU frame formats.

MSDUs is augmented. The major reason can be contributed to the inherent difference between the frame structures of A-MPDU and A-MSDU. As shown in Figure 1, each MPDU within an A-MPDU is associated with its own frame check sequence (FCS) for error correction. The frame error can be corrected on an MPDU basis, which results in monotonic increasing trend as shown in Figure 2(a); that is, the goodput performance will be enhanced as the number of aggregated MPDUs is enlarged.

On the other hand, a single FCS that exists within the frame structure of an MPDU will be utilized to conduct error correction for the entire A-MSDU. As the number of aggregated MSDUs is increased, there is no guarantee that the goodput performance will be enhanced owing to the existence of channel noises. In other words, the entire A-MSDU will be dropped while an uncorrectable error happens, which will decrease the transmission efficiency if the number of aggregated MSDUs has surpassed a certain limit. As can be seen from Figure 2(b), the goodput performance will be drastically decreased as the BER value is augmented. Based on the observations as above, it will be beneficial to obtain a feasible length of the MPDU payload (i.e., the l parameter as in Figure 1) such that the maximal goodput can be achieved under different SNR values. As will be shown in the next subsection, the optimal parameters, including both the MPDU payload size and the MCS scheme, will be acquired for achieving the maximal goodput under different channel conditions.

3.2. Goodput Analysis with Frame Aggregation. The analysis for saturation network goodput with the consideration of frame aggregation will be introduced in this subsection. In order to acquire the goodput performance based on the cross-layer information, two types of errors should be considered including both the modulation/demodulation errors and the decoding errors. First of all, the PHY layer BER is computed, which corresponds to the demodulation error caused by transmitting signals under an error-prone channel. Considering the MCS schemes described in the IEEE 802.11n standard, as shown in Table 1, three different modulation

Table 1: Modulation and coding schemes of the IEEE 802.11n standard.

MCS m_n	Modulation level	Code rate (R_c)	Data rate (Mbps)
1	BPSK	1/2	6.5
2	QPSK	1/2	13.0
3	QPSK	3/4	19.5
4	16-QAM	1/2	26.0
5	16-QAM	3/4	39.0
6	64-QAM	2/3	52.0
7	64-QAM	3/4	58.5
8	64-QAM	5/6	65.0

modes are utilized including BPSK, QPSK, and M-ary QAM. For BPSK and QPSK with code rate $R_c = 1/2$ and 3/4 (i.e., $m_n = 1, 2$, and 3 as in Table 1), the BER caused by the demodulation error $P_{be}(m_n)$ can be obtained from [24] as

$$P_{be}(m_n) = Q\left(\sqrt{2\frac{E_b}{N_0}}\right), \tag{1}$$

where the $Q(x)$ function represents the complementary Gaussian cumulative distribution function (CDF). The SNR value estimated at the receiver is denoted by E_b/N_0, where E_b is the energy per bit and N_0 represents the noise power spectral density. For the remaining 16-QAM and 64-QAM schemes, that is, $m_n = 4, 5, 6, 7$, and 8, the BER $P_{be}(m_n)$ can be acquired as

$$\begin{aligned} P_{be}(m_n) = {} & \frac{2\left(\sqrt{M}-1\right)}{\sqrt{M}\log_2\sqrt{M}} \cdot Q\left(\sqrt{\frac{2\log_2 M \cdot (E_b/N_0)}{M-1}}\right) \\ & + \frac{2\left(\sqrt{M}-2\right)}{\sqrt{M}\log_2\sqrt{M}} \cdot Q\left(\sqrt{\frac{3\log_2 M \cdot (E_b/N_0)}{M-1}}\right), \end{aligned} \tag{2}$$

where the parameter M is equal to either 16 or 64 representing the corresponding QAM scheme. Furthermore, the MAC layer BER that accounts for the decoding error is calculated as follows. The convolutional encoder [25, 26] as defined in the IEEE 802.11n standard is utilized associated with the generator polynomials $g_0 = (133)_8$ and $g_1 = (171)_8$, along with the constrain length $K = 7$. Since each information bit is encoded into two symbols with 7 bits individually, a total of 14 bits will be required for the encoding process. Therefore, the average BER $P_e(m_n)$ in MAC layer can be approximated and obtained under the coding rates equal to $R_c = 1/2$, 2/3, 3/4, and 5/6 as

$$\begin{aligned} & P_e(m_n) \\ & \cong \begin{cases} \frac{1}{14}[11\zeta_{10}(m_n) + 38\zeta_{12}(m_n) + 193\zeta_{14}(m_n)], & R_c = \frac{1}{2}, \\ \frac{1}{14}[\zeta_6(m_n) + 16\zeta_7(m_n) + 48\zeta_8(m_n)], & R_c = \frac{2}{3}, \\ \frac{1}{14}[8\zeta_5(m_n) + 31\zeta_6(m_n) + 160\zeta_7(m_n)], & R_c = \frac{3}{4}, \\ \frac{1}{14}[14\zeta_4(m_n) + 69\zeta_5(m_n) + 654\zeta_6(m_n)] & R_c = \frac{5}{6}. \end{cases} \end{aligned} \tag{3}$$

It is noted that (3) is approximated by taking the first three terms of the union bound [25, 26] for decoding error and is divided by 14 encoding bits. Considering that the Viterbi decoding with hard decision is adopted for the convolution code, the probability $\zeta_d(m_n)$ within (3) of an incorrect path chosen with the Hamming distance d is obtained as

$$\begin{aligned} & \zeta_d(m_n) \\ & = \begin{cases} \frac{1}{2}C_{d/2}^d P_{be}(m_n)^{d/2}[1-P_{be}(m_n)]^{d/2} \\ \quad + \sum_{k=d/2+1}^{d} C_k^d P_{be}(m_n)^k \\ \quad \times [1-P_{be}(m_n)]^{d-k}, & d = \text{even value}, \\ \zeta_d(m_n) = \sum_{k=(d+1)/2}^{d} C_k^d P_{be}(m_n)^k \\ \qquad \times [1-P_{be}(m_n)]^{d-k}, & d = \text{odd value}, \end{cases} \end{aligned} \tag{4}$$

where the BER $P_{be}(m_n)$ can be acquired from (1) and (2) based on their respective MCS schemes.

After obtaining the MAC layer BER $P_e(m_n)$ (as in (3)) with respect to the SNR value estimated at the receiver end, the saturated network goodput can be analyzed under a two-dimensional Markov chain backoff model. As shown in Figure 3, every backoff operation $(s(t), b(t))$ consists of two stochastic processes $s(t) \in [0, m]$ and $b(t) \in [0, W_i - 1]$. In a backoff operation, the process $s(t)$ indicates the backoff stage with the maximum stage m, which corresponds to the system retry limit. The process $b(t)$ denotes the backoff timer at the ith backoff stage with contention window size $W_i = 2^i \cdot W$ for $0 \le i \le m$, where $W_0 = W$ represents the minimal contention window size. In order to derive the stationary distribution of the backoff model as in Figure 3, the state-transition probability should first be obtained. The parameter p is introduced as the probability for receiving inaccurate packet at the receiver node. It is noted that the unsuccessful reception of data packets at the receiver is resulted from either the packet collision or the channel noises. Therefore, the transition probabilities, which are defined as $P(i_1, k_1 \mid i_0, k_0) \triangleq (s(t+1) = i_1, b(t+1) = k_1 \mid s(t) = i_0, k(t) = k_0)$, can be obtained as follows:

$$\begin{aligned} & P(i, k \mid i, k+1) = 1, \quad k \in [0, W_i - 2],\ i \in [0, m], \\ & P(i, k \mid i-1, 0) = \frac{p}{W_i}, \quad k \in [0, W_i - 1],\ i \in [1, m], \\ & P(0, k \mid i, 0) = \frac{1-p}{W_0}, \quad k \in [0, W_0 - 1],\ i \in [0, m-1], \\ & P(0, k \mid m, 0) = \frac{1}{W_0}, \quad k \in [0, W_0 - 1]. \end{aligned} \tag{5}$$

With the state-transition probabilities acquired from (5), the corresponding stationary distribution defined as $\pi_{i,k} \triangleq \lim_{t\to 0} P(s(t) = i,\ b(t) = k)$ with $i \in [0, m]$,$k \in [0, W_i - 1]$

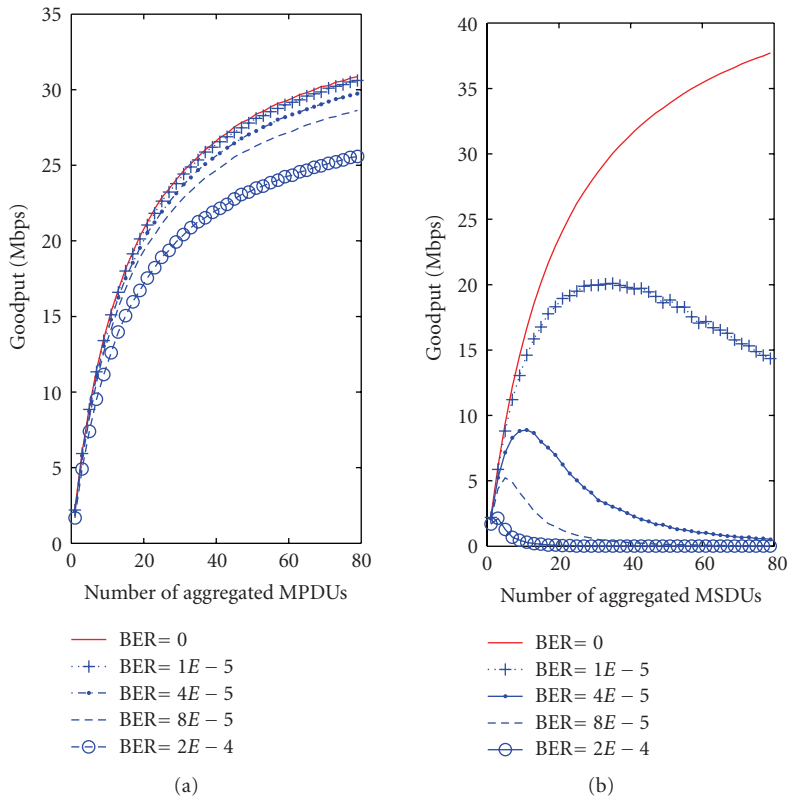

Figure 2: Goodput performance versus the number of aggregated MPDUs (a) and the number of aggregated MSDUs (b).

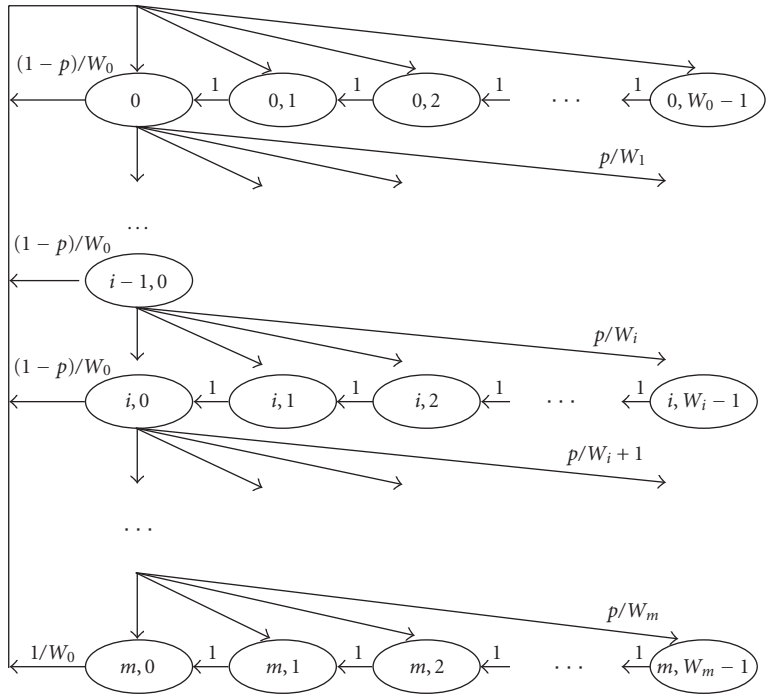

Figure 3: Two-dimensional Markov chain backoff model in consideration of packet collision and channel noises.

can be derived as follows:

$$\begin{aligned}
\pi_{i,0} &= \pi_{i-1,0} \cdot \sum_{k=0}^{W_i-1} \frac{p}{W_i} = \pi_{i-1,0} \cdot p \quad i \in [1,m] \\
\pi_{i,k} &= \pi_{i-1,0} \cdot \sum_{j=k}^{W_i-1} \frac{p}{W_i} \\
&= \pi_{i-1,0} \cdot p \cdot \frac{W_i - k}{W_i}, \quad i \in [1,m],\ k \in [0, W_i - 1] \\
\pi_{0,k} &= \frac{W_0 - k}{W_0} \cdot (1-p) \cdot \sum_{j=0}^{m-1} \pi_{j,0} \\
&\quad + \frac{W_0 - k}{W_0} \cdot \pi_{m,0}, \quad k \in [0, W_0 - 1]
\end{aligned} \tag{6}$$

In terms of $\pi_{0,0}$, the stationary distribution $\pi_{i,k}$, for all i,k in (6) can be expressed as

$$\begin{aligned}
\pi_{i,0} &= p^i \cdot \pi_{0,0}, \quad i \in [1,m] \\
\pi_{i,k} &= \frac{W_i - k}{W_i} \cdot \pi_{i,0}, \quad i \in [0,m],\ k \in [0, W_i - 1].
\end{aligned} \tag{7}$$

The characteristics of Markov chain model can be illustrated in (7) with probability p. The determination of probability p is shown as follows. Associated with the stationary cumulated distribution of Markov chain model; that is, $\sum_{i=0}^{m} \sum_{k=0}^{W_i-1} \pi_{i,k} = 1$, the state probability $\pi_{0,0}$ can be derived from (7) as

$$\begin{aligned}
\pi_{0,0} &= \left[\sum_{i=0}^{m} \sum_{k=0}^{W_i-1} p^i \cdot \frac{W_i - k}{W_i} \right]^{-1} \\
&= \frac{2(1-p)(1-2p)}{(1-p^{m+1})(1-2p) + W(1-p)\left[1 - (2p)^{m+1}\right]}.
\end{aligned} \tag{8}$$

Consequently, the probability of any transmission within a randomly selected time slot, that is, the conditional transmission probability τ, can be obtained from (8) as

$$\begin{aligned}
\tau &= \sum_{i=0}^{m} \pi_{i,0} = \pi_{0,0} \cdot \sum_{i=0}^{m} p^i \\
&= \frac{2(1-2p)}{(1-2p) + W(1-p)\left[1 - (2p)^{m+1}\right]}.
\end{aligned} \tag{9}$$

On the other hand, since the inaccurate receptions of packets are incurred from either packet collision or channel noises, the probability p in (9) can be acquired as

$$p = P_{\text{col}} + (1 - P_{\text{col}}) P_{fe,a}(m_n, l), \tag{10}$$

where P_{col} denotes the collision probability. The parameter $P_{fe,a}(m_n, l)$ indicates the error probability for the entire A-MPDU, which is a function of the MCS scheme m_n and the payload size l. Both P_{col} and $P_{fe,a}(m_n, l)$ can be expressed as

$$P_{\text{col}} = 1 - (1-\tau)^{\alpha - 1}, \tag{11}$$

$$P_{fe,a}(m_n, l) = \left[P_{fe,m}(m_n, l) \right]^{N_m}, \tag{12}$$

where α is the total number of contending nodes that intend to access the channel. $P_{fe,m}$ indicates the frame error rate (FER) of a single MPDU within a noisy channel, and N_m represents the total number of MPDUs within an A-MPDU. As in (12), the failure transmission is defined only if all the MPDUs within an A-MPDU is received with uncorrectable error. It is obvious to observe from (10) to (12) that the stage-transition probability p can also be expressed as a function of the conditional transmission probability τ. Based on the cross-relationship between the variables τ and p as in (9)–(12), the value of τ can consequently be obtained through numerically solving these nonlinear equations.

By extending the DCF scheme as described in [27–30] with the frame aggregation technique, the saturated network goodput can be acquired as follows. The saturated network goodput is defined as the ratio of the averaged successfully received payloads of an A-MPDU to the time required to successfully transmit an A-MPDU, that is,

$$G(m_n, l) = \frac{E[L_a]}{E[T_a]} = \frac{E[L_a]}{E[T_B] + E[T_S] + E[T_C] + E[T_E]}. \tag{13}$$

In order to emphasize the impact from different parameters that are selected in the proposed FALA algorithm, the saturated goodput in (13) is denoted as a function of both the MCS scheme m_n and the MPDU payload size l. A successfully transmitted A-MPDU indicates that at least one MPDU in it has been received either without error or with correctable error. Therefore, the parameter $E[L_a]$ in (13) can be acquired as

$$\begin{aligned}
E[L_a] &= \sum_{i=0}^{N_m} C_i^{N_m} \left[1 - P_{fe,m}(m_n, l)\right]^i \left[P_{fe,m}(m_n, l)\right]^{N_m - i} \cdot i \cdot l \\
&= N_m \cdot l,
\end{aligned} \tag{14}$$

where the dummy variable i denotes the number of successfully received MPDUs within an A-MPDU transmission attempt. Moreover, $E[T_B] = (1 - P_{\text{tr}}) \cdot \sigma$ indicates the average length of non-frozen backoff time in a time slot, where σ is defined as the size of a slot time [27]. The parameter P_{tr} is the probability that at least one transmission is occurred in the considered time slot, that is, $P_{\text{tr}} = 1 - (1-\tau)^{\alpha}$. The average durations in a time slot for the successful transmission $E[T_S]$, the failure transmission caused by channel noises $E[T_E]$, and the transmission with collisions $E[T_C]$ are obtained as follows:

$$E[T_S] = P_{\text{tr}} P_{\text{wc}} \left[1 - P_{fe,a}(m_n, l)\right] \cdot T_{\text{Suc}}, \tag{15}$$

$$E[T_E] = P_{\text{tr}} P_{\text{wc}} P_{fe,a}(m_n, l) \cdot T_{\text{Er}}, \tag{16}$$

$$E[T_C] = P_{\text{tr}} (1 - P_{\text{wc}}) \cdot T_{\text{Col}}, \tag{17}$$

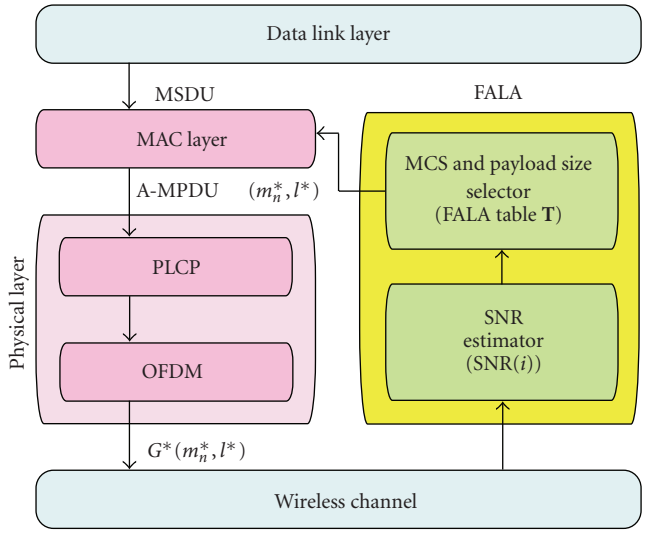

Figure 4: The system architecture for the proposed FALA algorithm.

where P_{wc} is the probability of transmission without collisions on condition that at leat one station is transmitting, that is,

$$P_{wc} = \frac{\alpha \cdot \tau \cdot (1-\tau)^{\alpha-1}}{P_{tr}} = \frac{\alpha \cdot \tau \cdot (1-\tau)^{\alpha-1}}{1-(1-\tau)^{\alpha}}. \quad (18)$$

According to the RTS/CTS scheme as described in [27], the time durations for successful and failure transmissions (as in (15) and (16)) are considered equal as $T_{Suc} = T_{Er} = T_{RTS} + T_{CTS} + T_{Header} + T_{Payload} + T_{BlockAck} + 3T_{SIFS} + 4\rho + T_{DIFS}$, where ρ represents the propagation delay. It is noted that the meaning for these timing parameters are denoted by their corresponding subscripts. The time interval for the occurrence of collision as in (17) is obtained as $T_{Col} = T_{RTS} + \rho + T_{DIFS}$. As a result, the saturated goodput $G(m_n, l)$ as in (13) based on specific values of the MPDU payload size l and the MCS scheme m_n can be acquired.

3.3. Implementation of FALA Algorithm. In this subsection, the implementation of proposed FALA algorithm will be explained. Figure 4 illustrates the schematic diagram for the realization of FALA scheme, which represents a cross-layer architecture. It is noticed that the original IEEE 802.11n standard will not be modified, where an additional link adaptor is imposed for the implementation of FALA algorithm.

The implementation of proposed FALA scheme is composed by both offline table construction and online adaption process. The first step is to establish the FALA table that maps from the SNR input to the output set (m_n^*, l^*), which indicates the optimal MCS scheme m_n^* and the optimal MPDU payload size l^* for achieving the maximal goodput performance. For implementation purpose, discrete sets of SNR values concerned in the FALA scheme will be utilized to facilitate the table construction. The SNR input obtained from the wireless channel will be grouped into specific ranges of values from SNR_{min} to SNR_{max} stepped by ΔS as

$$\mathbf{S}_i = \begin{cases} \left(-\infty, SNR_{min} + \frac{\Delta S}{2}\right), & i = 1, \\ \left[SNR(i) - \frac{\Delta S}{2}, SNR(i) + \frac{\Delta S}{2}\right), & 1 < i < n_s, \\ \left[SNR_{max} - \frac{\Delta S}{2}, \infty\right), & i = n_s, \end{cases} \quad (19)$$

where $SNR(i) = SNR_{min} + (i-1) \cdot \Delta S$ for $1 \le i \le n_s$, and $n_s = (SNR_{max} - SNR_{min})/\Delta S + 1$. Any SNR value that falls within the range of $\mathbf{S}_i$ will be approximated by the corresponding center value $SNR(i)$. Associated with the discretized set of SNR values, the saturated goodput value as derived in (13) can be obtained. The major limitation of the offline computation is on the granularity ΔS of SNR value. If the granularity ΔS is too large, the system goodput computed by the approximated center value $SNR(i)$ will deviate from the exact value. In order to acquire better approximation, the granularity ΔS should be kept small.

In the construction of FALA table, thanks to the small set of MCS schemes and the finite number of frame payload size, the computation for the corresponding maximum goodput performance can be easily executed on the conventional computer systems. Moreover, the computation time can even be ignored since the table is established in the offline manner. Therefore, the computation time will not be a concern for the FALA table construction, leading to the adoption of exhaustive search method. Based on the offline exhaustive search, the desired optimal link adapting parameter set $(m_n^*(i), l^*(i))$ can therefore be acquired under a given $SNR(i)$ value as

$$(m_n^*(i), l^*(i)) = \arg \max_{\forall m_n, l} G(m_n, l). \quad (20)$$

Consequently, the offline FALA table $\mathbf{T}$ can be constructed as $\mathbf{T} = [SNR(i), m_n^*(i), l^*(i)]$ for all $1 \le i \le n_s$. After the establishment of FALA table, the online adaptation phase can be initiated. As shown in Figure 4, the SNR estimator at the receiving end is utilized to estimate the SNR value from the wireless channel. The SNR value will consequently be fed into the FALA table $\mathbf{T}$ for the selection of optimal parameter set (m_n^*, l^*) in order to achieve the maximal goodput performance $G^*(m_n^*, l^*)$ under the given SNR value. The parameter set (m_n^*, l^*) will be provided to both the MAC and PHY layers of the conventional IEEE 802.11n protocol for the selection of feasible MPDU payload size and MCS scheme. It is also noted that the selection of MPDU payload size corresponds to the determination of the number of aggregated MSDUs within an A-MSDU. As a result, enhanced goodput performance can be achieved with adaptive selection of the system parameters m_n^* and l^*.

With the realization of pre-established FALA table, the pseudo code of FALA algorithm is shown in Algorithm 1. It can be seen that the conventional transmitting and receiving mechanisms of the IEEE 802.11 MAC protocol remain unchanged. Additional efforts are conducted in system runtime to keep trace of the channel conditions in

Table 2: System parameters for performance evaluation.

Simulation parameters	
RTS packet	20 Bytes
CTS packet	14 Bytes
Block Ack packet	32 Bytes
MAC Header	24 Bytes
PHY Header	24 Bytes
T_{SIFS}	16 μs
T_{DIFS}	34 μs
Propagation Delay (ρ)	1 μs
Slot_Time (σ)	9 μs
Retry Limit	7
Minimal Contention Window Size (W_0)	32
Maximal Contention Window Size (W_m)	4096

order to determine the optimal MCS scheme and the optimal MPDU payload size for the next transmission attempt. As was described, with the construction of offline table **T**, there is no additional calculation required for the proposed FALA algorithm to conduct realtime implementation.

4. Performance Evaluation

In this section, the performance of proposed FALA scheme will be evaluated and compared to both the ARF and the CLA algorithms via simulations. Error-prone channel is considered by adopting the binary symmetric model is for performance comparison. A C/C++ network simulation model is constructed by considering the access point-based single-hop communications. As shown in Table 2, the parameters described in the IEEE 802.11n standard are employed for both the construction of FALA table and the simulations. It is noted that the MAC header includes the MPDU header, the delimiter, and the FCS within the single MPDU of an A-MPDU as shown in Figure 1.

4.1. Construction of FALA Table. The offline construction of FALA table is illustrated in this subsection. The number of aggregated MPDUs is chosen as $N_m = 64$; while the payload size of a single MPDU l is selected to range from 10 to 5000 bytes. The SNR value in consideration is bounded within [$\text{SNR}_{\min} = -2$ dB, $\text{SNR}_{\max} = 18$ dB] stepped by $\Delta S = 0.25$ dB. As shown in Figure 5 with the adoption of FALA algorithm, the maximal achievable network goodput can be obtained under different SNR values, that is, by acquiring both optimal m_n^* and l^* from (20). On the other hand, the maximal achievable goodput by utilizing specific MCS schemes (i.e., $m_n = 1$ to 8) are also illustrated in Figure 5 for validation and comparison purposes, that is, by only obtaining optimal payload size l^* under the specific m_n value. Comparing with the eight MCS schemes, it is intuitive to observe that the proposed FALA scheme will result in the maximal goodput under different SNR values, that is, the outer profile integrated by the various MCS schemes as shown in Figure 5.

Based on Figure 5, the FALA table $\mathbf{T} = [\text{SNR}(i), m_n^*(i), l^*(i)]$ can be constructed with the data as shown in Figure 6. It can be observed that the optimal selections of both the MCS scheme m_n^* and the MPDU payload size l^* are acquired under specific SNR value, for example, $m_n^* = 5$ and $l^* = 1$ KByte under SNR = 10 dB. Different MCS schemes and MPDU payload sizes will be chosen from the proposed FALA scheme under various SNR values. In each specific range of SNR values with the same MCS scheme, the optimal MPDU payload size will be decreased as the SNR value is decremented. It is intuitive to conclude that the size of MPDU payload should be reduced if the channel condition becomes worse for data transmission. As the SNR value exceeds around 16 dB, the highest MCS scheme ($m_n^* = 8$) and the largest MPDU payload size ($l^* = 5$ KByte) are selected owing to the comparably better channel conditions. Furthermore, for comparison purpose, the maximal goodput that can be achieved by selecting the optimal MCS scheme with fixed MPDU payload size (i.e., with fixed value of $l = 5$ KByte) is also illustrated. It can be observed that with the adjustment of MPDU payload size l^*, a higher level of MCS scheme will be selected by the proposed FALA algorithm compared with that by adopting fixed MPDU payload size, for example, $m_n^* = 5$ for FALA scheme and $m_n^* = 4$ for fixed MPDU payload size under SNR = 10 dB.

4.2. Performance Comparison under Fixed Channel Conditions. Based on the offline constructed table as shown in Figure 6, performance comparison between the proposed FALA algorithm and the CLA scheme is conducted under fixed channel conditions. Figure 7 illustrates the comparison of goodput performance between these two algorithms under different SNR values ranging from -2 to 18 dB; while the corresponding MCS schemes adopted by both schemes are shown in Figure 8. It is noted that the number of aggregated MPDU is selected as $N_m = 64$ for both cases, and the MPDU payload size for the CLA scheme is chosen to be the maximum value as $l = 5$ KByte. It can be observed that both methods can achieve the same network goodput under better channel quality, that is, while the SNR value is greater than 14 dB. On the other hand, with the adjustable MPDU payload size l^*, the proposed FALA algorithm will result in higher goodput performance compared to the CLA scheme. By observing SNR = 10.5 dB as an example, the network goodput is equal to 30 Mbps for the FALA algorithm and 25 Mbps for the CLA scheme from Figure 7; while the corresponding MCS scheme is selected as $m_n = 5$ for the FALA algorithm and $m_n = 4$ for the CLA method as shown in Figure 8. Moreover, as the SNR value is incremented, it is observed from Figure 8 that the MCS scheme obtained from the FALA algorithm will be switched to a higher data rate earlier than the CLA method. With the flexibility to choose both the MCS scheme and the MPDU payload size, the proposed FALA algorithm can achieve higher network goodput, especially under the channel conditions with lowered SNR values.

Pre-establishment of FALA table $\mathbf{T} = [\mathrm{SNR}(i), m_n^*(i), l^*(i)]$;
l_c: the MPDU payload size in the current transmission attempt of an A-MPDU;
$m_{n,c} = m_1$: the initial MCS scheme in the current transmission attempt;
$m = 7$: the retry limit;
while *the queue of data packet is nonempty* **do**
  count_success = 0;
  count_fail = 0;
  $n_c = 0$, the count of transmission attempts;
  SNR_c: the channel condition in the current transmission attempt;
  obtain $m_{n,c} = m_n^*$ and $l_c = l^*$ based on the FALA table **T** and SNR_c;
  (the first N_m frames at the head of data queue are transmitted as an A-MPDU);
  if *an A-MPDU is received* **then**
    for*all* N_m *MPDUs* **do**
      (check all N_m MPDUs in the A-MPDU, and remove *count_success* successfully transmitted frames in the data queue);
      if *an MPDU in the A-MPDU is received without error* **then**
        count_success = *count_success* + 1;
      else
        count_fail = *count_fail* + 1;
    if *count_success* = 0 **then**
      (this indicates that the entire N_m MPDUs are received with error);
      $n_c = n_c + 1$;
      count_success = 0;
      count_fail = 0;
  if $n_c > m$ **then**
    (the N_m frames in the data queue are dropped);
    $n_c = 0$;
    count_success = 0;
    count_fail = 0;

Algorithm 1: Proposed Frame-Aggregated Link Adaptation (FALA) Algorithm.

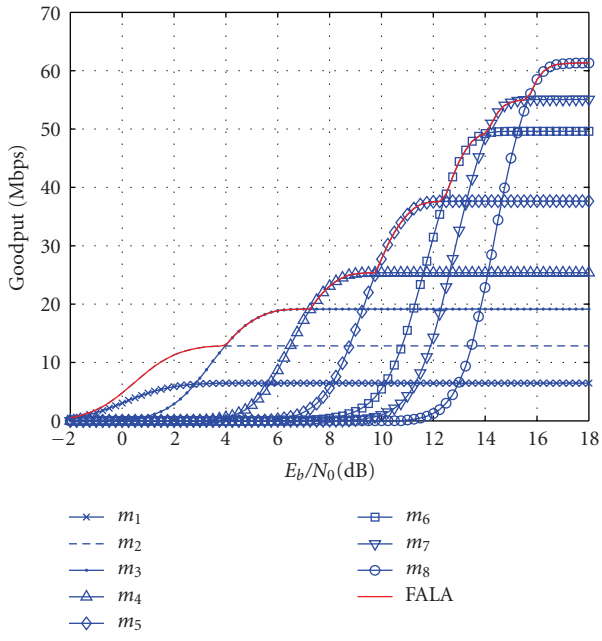

Figure 5: Maximal achievable goodput performance by adopting FALA algorithm and the eight MCS schemes.

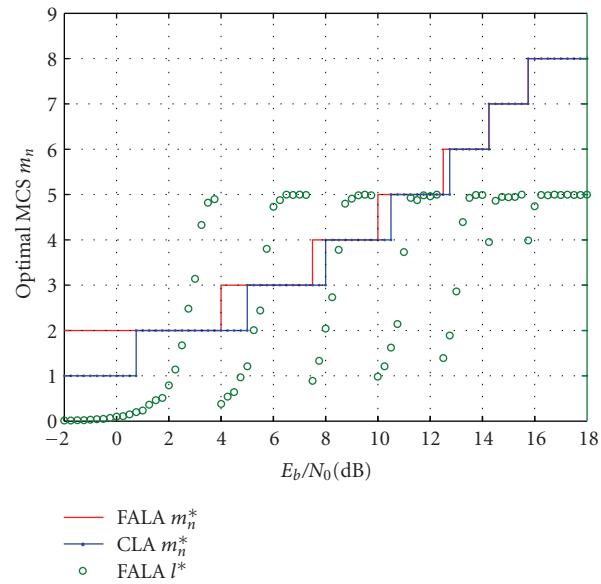

Figure 6: The FALA table **T**: optimal selections of the MCS scheme m_n^* (left axis) and the MPDU payload size l^* (right axis) versus the SNR value. The optimal MCS schemes with fixed MPDU payload size ($l = 5$ KBytes) is also illustrated for comparison purpose.

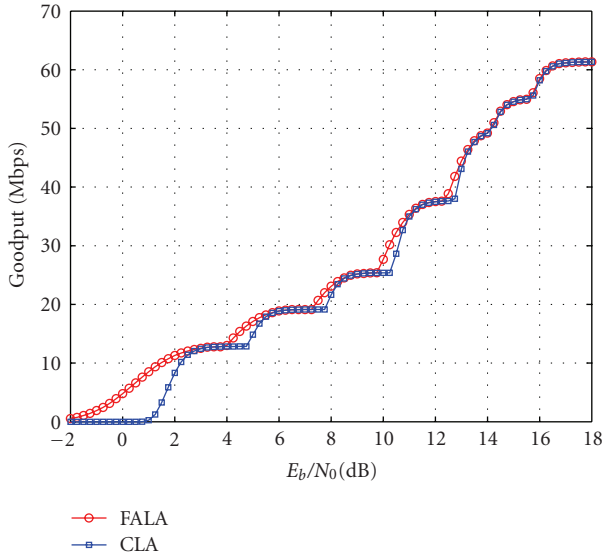

Figure 7: Performance comparison: goodput versus SNR value. The MPDU payload size for FALA algorithm $l \in [10, 5000]$, and MPDU payload size for CLA scheme $l = 5000$ bytes.

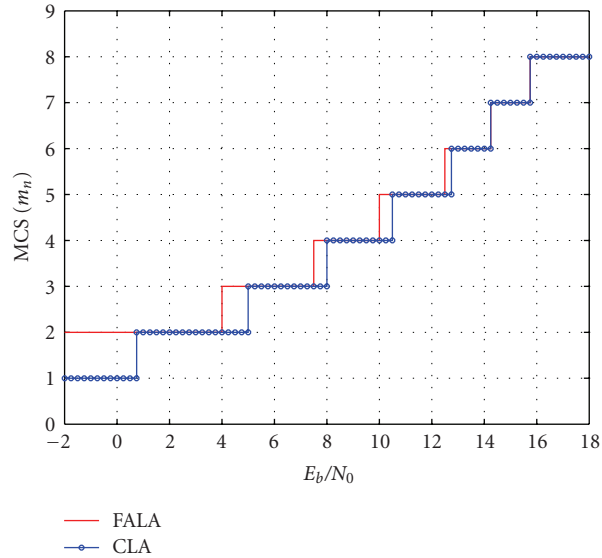

Figure 8: The corresponding MCS schemes versus SNR values adopted in the goodput comparison as in Figure 7.

4.3. Performance Comparison under Variable Channel Conditions. In this subsection, the performance comparison between the FALA, the ARF, and the CLA algorithms are conducted under time-varying channels. In order to compare and verify the adaptability to the channel variations, the discrete Markov chain model [21, 31] is suggested. The Markov chain model specified in [31] for the SNR variation is constructed by the trace collection of the packet SNR measurement. The trace collection can be viewed as the training input for this model. Based on the model testing, the eight-state model shows its accuracy to measure the channel variations represented by the trace collection. However, due to the lack of the training source of the packet SNR measurement, the measurement-based model in [31] can not be established in our protocol evaluation.

As shown in Figure 9, a simple two-state discrete Markov chain [21] is therefore utilized to model the channel variations. The channel is considered to compose two different conditions denoted as good and bad states. Within good channel condition, the SNR value is uniformly distributed from 8 to 18 dB; while it is uniformly distributed from -2 to 8 dB under bad channel condition. The probabilities $P_{b,g}$, $P_{g,b} = 1 - P_{b,g}$, $P_{b,b} = 1 - P_{b,g}$, and $P_{g,g} = P_{b,g}$ indicate either the channel-varying probability between good and bad conditions or the probability to stay in the same condition. For example, a probability $P_{b,g} = 0.7$ indicates that the channel condition will vary from bad to good with 70% of probability. A larger value of $P_{b,g}$ indicates that there are higher probability for the channel to be changed into a better condition.

Figure 10 shows the performance comparison between the ARF and the FALA algorithms under the time-varying channel. The channel conditions within different transmission attempts generated by the two-state discrete Markov chain model with $P_{b,g} = 0.7$ is illustrated in Figure 10(a).

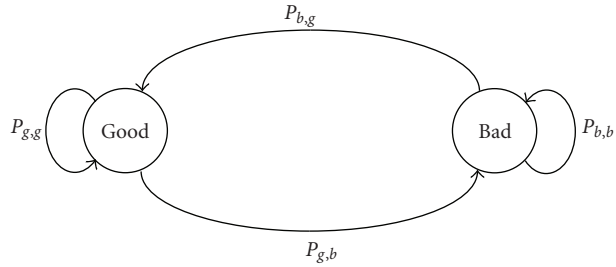

Figure 9: A two-state discrete Markov chain model for channel variations.

The MCS scheme adopted by the ARF algorithm in every transmission attempt is shown in Figure 10(b); while Figure 10(c) illustrates the MCS scheme exploited by the proposed FALA algorithm. It can be observed that the proposed FALA scheme (Figure 10(c)) can provide better adaptability to channel variations compared to the ARF algorithm (Figure 10(b)). The major reason is contributed to the adoption of cross-layer information by using the FALA scheme, including both the MCS scheme and the MPDU payload size. An optimal MCS scheme will always be selected by the proposed FALA algorithm under channel variations. On the other hand, the ARF method merely employs the MAC timers to record consecutive successful or failed transmission attempts for the determination of its packet retransmissions. The resulting slow adaptation by employing the ARF scheme is observed incapable to trace the fast-changing channel conditions.

Figure 11 illustrates the performance comparison between the FALA, the ARF, and the CLA algorithms under different channel variations with the probability $P_{b,g}$ ranging from 0 to 1. It is noted that the goodput performance by adopting merely the MCS schemes $m_n = 1$ and $m_n = 8$ (as in Table 1) is also illustrated for comparison purpose. It is

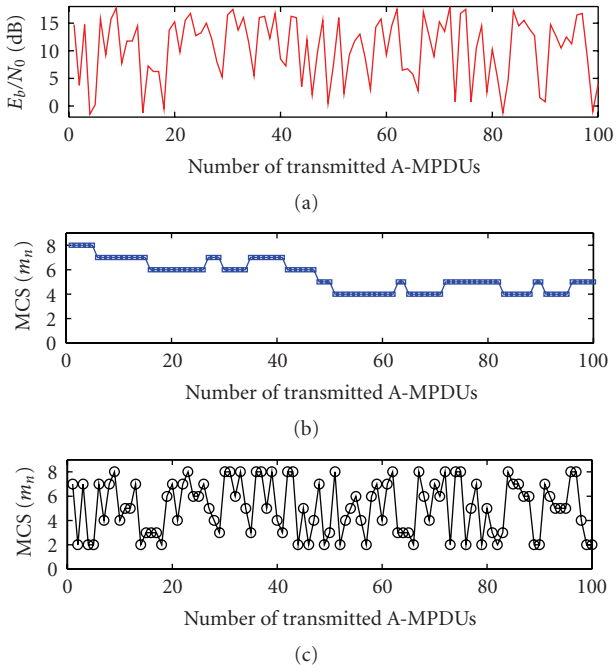

FIGURE 10: (a) the channel conditions within different transmission attempts generated by the two-state discrete Markov chain model with $P_{b,g} = 0.7$. (b) the MCS scheme adopted by the ARF algorithm in every transmission attempt. (c) the MCS scheme exploited by the proposed FALA algorithm in every transmission attempt.

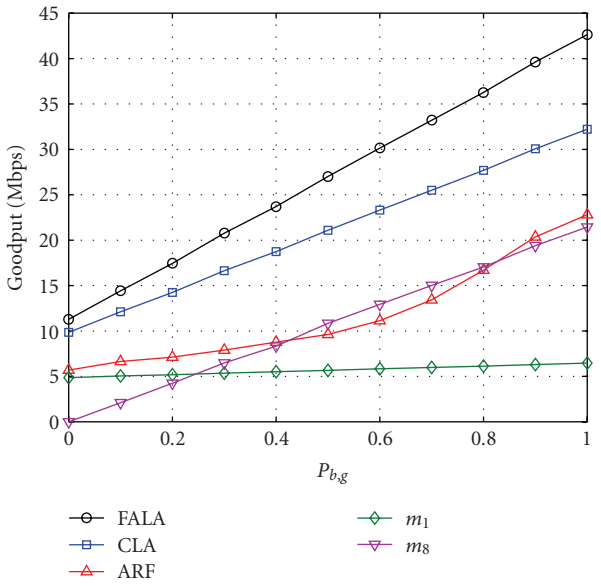

FIGURE 11: Performance comparison: average goodput versus channel variations with $P_{b,g}$ from 0 to 1.

reasonable to see that the MCS scheme with lowered data rate (i.e., $m_n = 1$) offers better performance comparing with that with $m_n = 8$ under worse channel conditions, that is, with smaller values of $P_{b,g}$. As the channel condition becomes better, the goodput performance associated with $m_n = 8$ will outperform that with $m_n = 1$ by providing higher data rate for packet transmission. Owing to the adaptation of MCS schemes, the CLA algorithm can provide better goodput performance compared to the ARF method, for example, goodput = 28 Mbps for the CLA algorithm and goodput = 18 Mbps for the ARF scheme under $P_{b,g} = 0.8$. Furthermore, it can be observed that the proposed FALA algorithm outperforms all the other existing schemes under different channel conditions, for example, goodput = 36 Mbps for the FALA algorithm and goodput = 28 Mbps for the CLA scheme under $P_{b,g} = 0.8$. The major reason is contributed to its adaptation to both the MCS scheme and the MPDU payload size for achieving the maximal goodput performance. The merits of proposed FALA protocol can therefore be observed.

5. Conclusion and Future Work

In this paper, a frame-aggregated link adaptation (FALA) protocol is proposed to maximize the network goodput performance from the cross-layer perspective. Instead of simply utilizing the PHY-layer modulation and coding schemes (MCS), the proposed FALA protocol further considers the effects from the MAC-layer optimal payload size based on frame aggregation. With the additional consideration of adjustable payload size, the network goodput can be effectively improved under different signal-to-noise ratios (SNRs). Numerical results show that with the increase of SNR values and the optimal selection of payload size, the proposed FALA algorithm can change to higher MCS schemes faster than the baseline algorithms, leading to higher goodput performance. In the simulation-based performance evaluation, it shows and validates that the proposed FALA algorithm outperforms the existing link adaptation schemes in the network goodput performance, especially under the environments with time-varying channels. Protocol realization on a hardware platform and the validation of field experiments will be included in our future work.

Acknowledgment

This paper was in part funded by the Aiming for the Top University and Elite Research Center Development Plan, NSC 96-2221-E-009-016, NSC 98-2221-E-009-065, the MediaTek research center at National Chiao Tung University, the Universal Scientific Industrial (USI) Co., and the Telecommunication Laboratories at Chunghwa Telecom Co. Ltd, Taiwan.

References

[1] IEEE 802.11 WG, "IEEE Std 802.11a-1999(R2003): Part 11: Wireless LAN Medium Access Control (MAC) and Physical Layer (PHY) specifications: High-speed Physical Layer in the 5 GHz Band," IEEE Standards Association Std., 2003.

[2] IEEE 802.11 WG, "IEEE Std 802.11b-1999(R2003): Part 11: Wireless LAN Medium Access Control (MAC) and Physical Layer (PHY) specifications: Higher-Speed Physical Layer Extension in the 2.4 GHz Band," IEEE Standards Association Std., 2003.

[3] IEEE 802.11 WG, "IEEE Std 802.11g-2003: Part 11: Wireless LAN Medium Access Control (MAC) and Physical Layer (PHY) specifications: Amendment 4: Further Higher Data Rate Extension in the 2.4 GHz Band," IEEE Standards Association Std., 2003.

[4] IEEE 802.11 WG, "IEEE Std 802.11e-2005: Part 11: Wireless LAN Medium Access Control (MAC) and Physical Layer (PHY) specifications: Amendment 8: Medium Access Control (MAC) Quality of Service Enhancements," IEEE Standards Association Std., 2005.

[5] EWC, "HT MAC Specification, Interoperability MAC Specification v1.24," Enhanced Wireless Consortium Std., January 2006.

[6] IEEE 802.11 WG, "IEEE P802.11n/D3.00: Part 11: Wireless LAN Medium Access Control (MAC) and Physical Layer (PHY) specifications: Amendment 4: Enhancements for Higher Throughput," IEEE Standards Association Std., September 2007.

[7] Y. Li, S.-W. Kim, J.-K. Chung, and H.-G. Ryu, "SFBC-based MIMO OFDM and MIMO CI-OFDM systems in the nonlinear and NBI channel," in *Proceedings of the International Conference on Communications, Circuits and Systems (ICCCAS '06)*, pp. 898–901, June 2006.

[8] Y. Li, X. Wang, and S. A. Mujtaba, "Impact of physical layer parameters on the MAC throughput of IEEE 802.11 wireless LANs," in *Proceedings of the 38th Asilomar Conference on Signals, Systems and Computers*, pp. 1468–1472, November 2004.

[9] D. Skordoulis, Q. Ni, H.-H. Chen, A. P. Stephens, C. Liu, and A. Jamalipour, "IEEE 802.11N MAC frame aggregation mechanisms for next-generation high-throughput WLANs," *IEEE Wireless Communications*, vol. 15, no. 1, Article ID 4454703, pp. 40–47, 2008.

[10] S. Kim, S.-J. Lee, and S. Choi, "The impact of IEEE 802.11 MAC strategies on multi-hop wireless mesh networks," in *Proceedings of the 2nd IEEE Workshop on Wireless Mesh Networks (WiMESH '06)*, pp. 38–47, September 2006.

[11] D. Skordoulis, Q. Ni, U. Ali, and M. Hadjinicolaou, "Analysis of concatenation and packing mechanisms in IEEE 802.11n," in *Proceedings of the 6th Annual Postgraduate Symposium on the Convergence of Telecommunications, Networking and Broadcasting (PGNET '07)*, 2007.

[12] B. Ginzburg and A. Kesselman, "Performance analysis of A-MPDU and A-MSDU aggregation in IEEE 802.11n," in *Proceedings of the IEEE Sarnoff Symposium (SARNOFF '07)*, pp. 1–5, May 2007.

[13] Y. Kim, S. Choi, K. Jang, and H. Hwang, "Throughput enhancement of IEEE 802.11 WLAN via frame aggregation," in *Proceedings of the IEEE 60th Vehicular Technology Conference (VTC '04)*, pp. 3030–3034.

[14] Y. Chang, C. Lee, B. Kwon, and J. Copeland, "Dynamic optimal fragmentation for goodput enhancement in WLANs," in *Proceedings of the International Conference on Testbeds and Research Infrastructure for the Development of Networks and Communities (TridentCom '07)*, pp. 1–9, 2007.

[15] Q. Ni, T. Li, T. Turletti, and Y. Xiao, "Mac layer proposal for IEEE 802.11n: frame aggregation with fragment retransmission (AFR) scheme," IEEE 802.11n Working Group Standard Draft No. IEEE 802.11-04-0950-00-000n, August 2004.

[16] T. Li, Q. Ni, D. Malone, D. Leith, Y. Xiao, and T. Turletti, "Aggregation with fragment retransmission for very high-speed WLANs," *IEEE/ACM Transactions on Networking*, vol. 17, no. 2, pp. 591–604, 2009.

[17] Y. Xiao, "Packing mechanisms for the IEEE 802.11n wireless LANs," in *Proceedings of the IEEE Global Telecommunications Conference (GLOBECOM '04)*, pp. 3275–3279, November 2004.

[18] Y. Lu, C. Zhang, J. Lu, and X. Lin, "A MAC queue aggregation scheme for VoIP transmission in WLAN," in *Proceedings of the IEEE Wireless Communications and Networking Conference (WCNC '07)*, pp. 2123–2127, March 2007.

[19] K. Lee, S. Yun, I. Kang, and H. Kim, "Hop-by-hop frame aggregation for VoIP on multi-hop wireless networks," in *Proceedings of the IEEE International Conference on Communications (ICC '08)*, pp. 2454–2459, May 2008.

[20] A. Kamerman and L. Monteban, "WaveLAN®-II: a high-performance wireless LAN for the unlicensed band," *Bell Labs Technical Journal*, vol. 2, no. 3, pp. 118–133, 1997.

[21] D. Qiao, S. Choi, and K. G. Shin, "Goodput analysis and link adaptation for IEEE 802.11 a wireless LANs," *IEEE Transactions on Mobile Computing*, vol. 1, no. 4, pp. 278–292, 2002.

[22] J. D. P. Pavon and S. Choi, "Link adaptation strategy for IEEE 802.11 WLAN via received signal strength measurement," in *Proceedings of the International Conference on Communications (ICC '03)*, vol. 2, pp. 1108–1113, May 2003.

[23] Y. Nagai, A. Fujimura, M. Akihara et al., "A closed-loop link adaptation scheme for 324Mbit/sec WLAN system," in *Proceedings of the 18th Annual IEEE International Symposium on Personal, Indoor and Mobile Radio Communications (PIMRC '07)*, September 2007.

[24] J. G. Proakis, *Digital Communication*, MacGraw-Hill, New York, NY, USA, 4th edition.

[25] J. Conan, "The weight spectra of some short low-rate convolution codes," *IEEE Transactions on Communications*, vol. 32, no. 9, pp. 1050–1053, 1984.

[26] D. Haccoun and G. Begin, "High-rate punctured convolutional codes for Viterbi and sequential decoding," *IEEE Transactions on Communications*, vol. 37, no. 11, pp. 1113–1125, 1989.

[27] G. Bianchi, "Performance analysis of the IEEE 802.11 distributed coordination function," *IEEE Journal on Selected Areas in Communications*, vol. 18, no. 3, pp. 535–547, 2000.

[28] P. Chatzimisios, A. C. Boucouvalas, and V. Vitsas, "Performance analysis of IEEE 802.11 DCF in presence of transmission errors," in *Proceedings of the IEEE International Conference on Communications (ICC '04)*, pp. 3854–3858, June 2004.

[29] Z. Hadzi-Velkov and B. Spasenovski, "Saturation throughput—delay analysis of IEEE 802.11 DCF in fading channel," in *Proceedings of the International Conference on Communications (ICC '03)*, pp. 121–126, May 2003.

[30] Q. Ni, T. Li, T. Turletti, and Y. Xiao, "Saturation throughput analysis of error-prone 802.11 wireless networks," *Wireless Communications and Mobile Computing*, vol. 5, no. 8, pp. 945–956, 2005.

[31] R. K. Guha and S. Sarkar, "Characterizing temporal SNR variation in 802.11 networks," *IEEE Transactions on Vehicular Technology*, vol. 57, no. 4, pp. 2002–2013, 2008.